Annals of Nuclear Medicine Vol. 6, No. 4, 253–260, 1992

Single photon emission computed tomography using ^{201}Tl chloride in pulmonary nodules: comparison with ^{67}Ga citrate and ^{99m}Tc-labeled hexamethyl-propyleneamine-oxime

Kazuo ITOH,* Hironori TAKEKAWA,** Eriko TSUKAMOTO,* Kazuhiko NAGAO,* Kunihiro NAKADA,* Shosaku ABE,** Yoshikazu KAWAKAMI** and Masayori FURUDATE*

*Departments of *Nuclear Medicine and **First Department of Internal Medicine, Hokkaido University School of Medicine*

A single photon emission computed tomography (SPECT) with ^{201}Tl chloride (Tl-201) was carried out prospectively in 50 patients with pulmonary nodules and its diagnostic value was compared with those of ^{67}Ga citrate (Ga-67) and ^{99m}Tc-labeled hexamethyl-propyleneamine-oxime (Tc-99m-HMPAO). Tl-201 SPECT provided 88% (early)–91% (delayed) sensitivity, 85% (early and delayed) specificity and 87% (early)–89% (delayed) accuracy. The sensitivity of the Tl-201 planar image was 56 (early)–62% (delayed), which was significantly lower than that of SPECT. Delayed SPECT images at 2 hour postinjection were more preferable to disclose the malignant pulmonary nodule than early SPECT images at 15 minutes postinjection. The application of SPECT with Ga-67 failed to improve the sensitivity of planar imaging for malignant pulmonary nodules. Tc-99m-HMPAO was concentrated in 62% of 13 patients with malignant pulmonary nodules, which was slightly higher than Ga-67 in 54% of 28 patients. In an analysis of the histologic types of lung cancer, the sensitivity of Tl-201 was not significantly different in all types. On the other hand, Ga-67 was positive only in 25% of 12 patients with adenocarcinoma.

A combination of SPECT and Tl-201 is the best choice among routine scintigraphic techniques for depicting malignant pulmonary nodules. The Tl-201 SPECT image may play a complementary role in the characterization of pulmonary nodules which are revealed on a plain radiograph and computed tomography.

Key words: single photon emission computed tomography (SPECT), ^{201}Tl chloride, ^{67}Ga citrate, ^{99m}Tc-hexamethyl-propyleneamine-oxime, lung cancer

INTRODUCTION

SCINTIGRAPHIC TECHNIQUES with tumor-specific radiolabeled immunoglobulin and positron labeled metabolites have been expected to be promising methods to characterize a solid mass but their clinical use is still limited.[1] ^{67}Ga citrate (Ga-67) is one of the most popular tumor-seeking radioagents, and has been widely used for the detection of various types of malignant tumors.[2–4] In our previous study of 153 cases of lung cancer,[5] Ga-67 provided a high true positive rate of 93% when the tumor was more than 3 cm in diameter. However, when the tumor was less than 3 cm in diameter, the sensitivity was as low as 33%. In addition, the positive prediction tended to depend on the histologic type of the lung cancer: it was highest in squamous cell carcinoma and lowest in adenocarcinoma.

Recent advances in single photon computed tomography (SPECT) have made a major impact on the non-invasive functional analysis of several organs, particularly the myocardium, brain, bones and kidneys. It may be expected to play a significant role in tumor prediction with combination of tumor-

Received April 3, 1992, revision accepted May 25, 1992.

For reprints contact: Kazuo Itoh, M.D., Department of Nuclear Medicine, Hokkaido University School of Medicine, Kita-15, Nishi-7, Kita-ku, Sapporo 060, JAPAN.

seeking radioagents.[6] Tonami et al.[7,8] applied ^{201}Tl chloride (Tl-201) to the investigation of lung cancer and concluded that a combination of Tl-201 and SPECT seems to be useful in detecting lung cancer and in differentiating malignant from benign lesions. Tl-201 is a biochemical analog of potassium and is taken up by myocardial cells through the same pathway as potassium.[9] Although the exact mechanism of Tl-201 uptake in tumors is still unclear, it has been adopted to depict malignant and benign neoplasms in the thyroid,[10] parathyroid[11,12] and brain.[13]

The lipophilic ^{99m}Tc-labeled hexamethyl-propyl-eneamine-oxime (Tc-99m-HMPAO) is a cerebral blood flow tracer that has been used primarily in patients with cerebral vascular disease.[14] Tc-99m-HMPAO has been shown to be concentrated in malignant tumors,[15,16] although it is still unclear whether this new radioagent has the same retention mechanism for malignant tumors as for normal tissue.

The primary aim of this study was to discuss the clinical value of SPECT with Tl-201 in pulmonary nodules in comparison with that of Ga-67. In addition, the clinical feasibility of Tc-99m-HMPAO for the positive delineation of pulmonary tumors was investigated.

MATERIALS AND METHODS

Patients

Fifty patients (male to female ratio, 30 to 20, age range 32 to 80 years and mean age 62 years) who had nodular shadows on a plain radiograph were prospectively investigated by means of Tl-201 SPECT. Final diagnosis of nodules was made by cytology of bronchial washing and/or histopathology of bronchoscopic biopsy, lobectomy and pneumonectomy. These included 36 patients with primary lung cancer (untreated 31, during chemotherapy 3, recurrent 1, and post-operative in disease-free state 1), 2 with metastatic lung cancer, and 14 with benign pulmonary and mediastinal diseases (Table 1). Ga-67 and Tc-99m-HMPAO scans which were carried out within 3 weeks before and after the Tl-201 study were referred to for comparison. Ga-67 in 41 patients and Tc-99m-HMPAO in 14 were included in this study.

Methods

Tl-201 SPECT was performed twice 15 min (early) and 2 hour (delayed) after i.v. injection of 3 mCi (111 MBq) of Tl-201 chloride. A gamma camera (GE-Maxi 400AT/C) equipped with a low-energy general-purpose parallel-hole collimator was interfaced with a dedicated computer (Starcam II). The dual peaks of emitted energy, 60–98 keV and 152–186 keV, were selected for data acquisition. The patient was placed in a supine position. The detector focusing the chest was rotated about 6 degrees at a time for a total of 360 degrees and image data were collected for 30 sec at each stop. A 128×128 matrix was used for data acquisition, and transaxial images were reconstructed by means of a Hanning pre-filter and Ramp post-filter. All reconstructed images were assembled with geographic attenuation correction using an effective linear attenuation coefficient of -0.19. Coronal and sagittal section images were assembled from transaxial images. 1.2 cm thick slices were further assembled for visual evaluation of the nodular uptake of Tl-201. Two planar images of anterior and posterior projections, containing 900,000 counts each, were also obtained before or after SPECT.

Ga-67 SPECT was performed 48–72 hour after i.v. injection of 2–3 mCi (74–111 MBq) of Ga-67 citrate. The same gamma camera with a medium-energy collimator was used and three-peak windows for gamma rays emitted from Ga-67 were set for data acquisition. The other methods for data acquisition were the same as for Tl-201 imaging.

Tc-99m-HMPAO SPECT images were obtained 5 min (early) and 4.5 hour (delayed) after i.v. injection of 20 mCi (740 MBq) immediately after labeling with Tc-99m pertechnetate. The gamma camera used was a Toshiba-602A equipped with the low-energy

Table 1 Final diagnosis in the population studied

Final diagnosis	Number of cases
Malignant pulmonary diseases	38
Primary pulmonary cancer	36
Untreated	31
During chemotherapy	3
Recurrent	1
Post-operative	1
Metastatic tumor	2
Melanoma	1
Adenocarcinoma	1
Benign pulmonary diseases	6
Pyothorax	1
Pleuritis	1
Old-tuberculosis	1
Bronchiectasis	1
Pneumonia	1
Hamartoma	1
Mediastinal tumor	5
Thymic cyst	2
Thymic carcinoid	1
Schwannoma	1
Intrathoracic goiter	1
Schwannoma of the chest wall	1
Total	50

high-resolution parallel-hole collimator. The gamma ray energy of 140 keV ±10% was selected and the detector was rotated 6 degrees at a time for a total of 360 degrees and stopped for 20 sec each time. Images were reconstructed by the means of 3 point pre-smoothing and Shepp and Logan post-filters.

Geographic localization of a focal uptake of the administered radiotracer by the pulmonary nodule was evaluated with reference to findings in both the chest radiograph (CTX) and CT scan. When the uptake of the radiotracer in nodules was equal to or less than in the background, then it was interpreted as negative. When the nodular uptake was found to be slightly increased, the finding was considered as equivocal. When the nodular uptake was clearly demonstrated, then the study was considered as positive. When the uptake in the target areas was defined as positive, scintigraphy was evaluated as positive.

For positive images, variable regions of interest (ROI) in the coronal or transaxial section image of SPECT were assigned over the nodular uptake area and background lung field around the nodular uptake or in the opposite lung field. Then the nodule-to-background ratio (Nodule/BG ratio) was calculated by means of a computer. It was expressed as the ratio of mean radioactivity in the nodular target ROI divided by mean radioactivity in the background ROI.

RESULTS

Analysis on sensitivity and specificity

Three patients with small cell carcinoma had already received chemotherapy when Tl-201 SPECT was performed. Two of them were positive but were excluded from the analysis. The sensitivity of Tl-201 SPECT in 34 malignant sites in 31 untreated cases, one having double cancer small cell carcinoma and adenocarcinoma, and 1 recurrent case, with double cancer small cell carcinoma and squamous cell carcinoma, was 88% in the early image and 91% in the delayed image (Table 2). Only one case with alveolar cell carcinoma became positive in delayed SPECT. Three false negative cases in delayed images included 1 with alveolar cell cancer and two with adenocarcinoma. There were two benign nodules which showed positive findings: 1 with a carcinoid tumor in the right upper mediastinal region and 1 with an intrathoracic goiter. Therefore, the specificity of Tl-201 was calculated to be 85% by adding a post-operative case of a disease-free state to 12 cases with a benign nodule. On the other hand, planar Tl-201 images provided 56–62% sensitivity and 85% specificity. The sensitivity of Tl-201 planar and SPECT images was significantly different in the statistical analysis ($p<0.01$). No study which showed planar positive and SPECT negative was encountered.

Three out of 41 patients with Ga-67 were given chemotherapy. These patients were excluded from the analysis. In 8 patients, whole body and planar scans were done instead of SPECT. Ga-67 SPECT did not enable improve the positive delineation of a solitary pulmonary nodule. Eight planar studies were included in the analysis. The sensitivity of Ga-67 scintigraphy in 38 patients with malignant pulmonary tumors was 53% and the specificity was 100%. The low sensitivity was mainly due to high false negatives in adenocarcinoma.

Fifteen out of 16 cases with Tc-99m-HMPAO had untreated primary pulmonary cancer. The sensitivity of this agent was 62%. Tc-99m-HMPAO SPECT was positive in one patient with pneumonia.

Analysis of factors on positive delineation with Tl-201

In squamous cell carcinoma (Fig. 1), all Tl-201 SPECT and 80% of Ga-67 scintigraphy results were positive. The positive rate of 50% in Tc-99m-HMPAO SPECT was lowest in squamous cell carcinoma (Table 3). In adenocarcinoma (Fig. 2), the

Table 2 Results of Tl-201, Ga-67 and Tc-99m-HMPAO scintigraphy in pulmonary nodules

Methods	Sensitivity	Specificity	Accuracy	Predictive value	
				Positive	Negative
Tl-201 Planar					
Early	56% (19/34)	85% (11/13)	64% (30/47)	90% (19/21)	42% (11/26)
Delayed	62% (21/34)*	85% (11/13)	70% (33/47)	91% (21/23)	46% (11/24)
Tl-201 SPECT					
Early	88% (30/34)	85% (11/13)	87% (41/47)	94% (30/32)	73% (11/15)
Delayed	91% (31/34)*,**	85% (11/13)	89% (42/47)	94% (31/33)	79% (11/14)
Ga-67 SPECT & Planar	54% (15/28)**	100% (11/11)	66% (26/39)	100% (15/15)	46% (11/24)
Tc-99m-HMPAO SPECT & Planar	62% (8/13)	0% (0/1)	57% (8/14)	89% (8/9)	0% (0/4)

*,**: statistically significant ($p<0.01$)

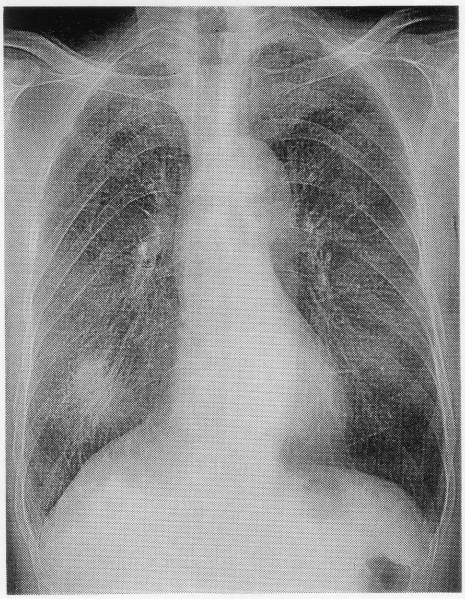

A

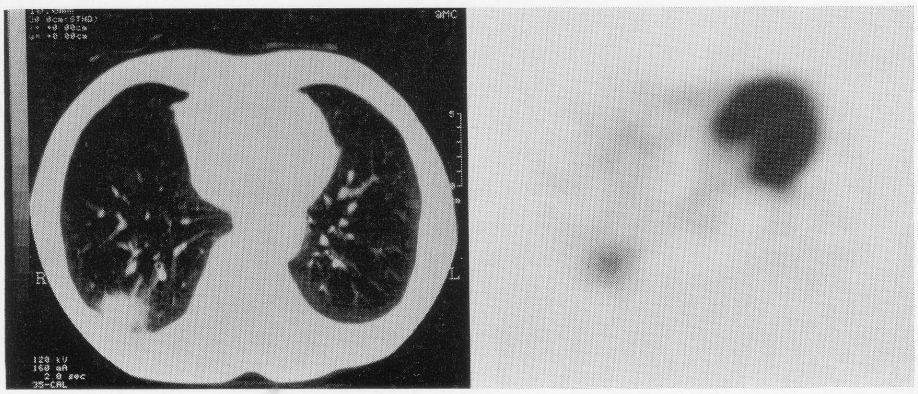

B C

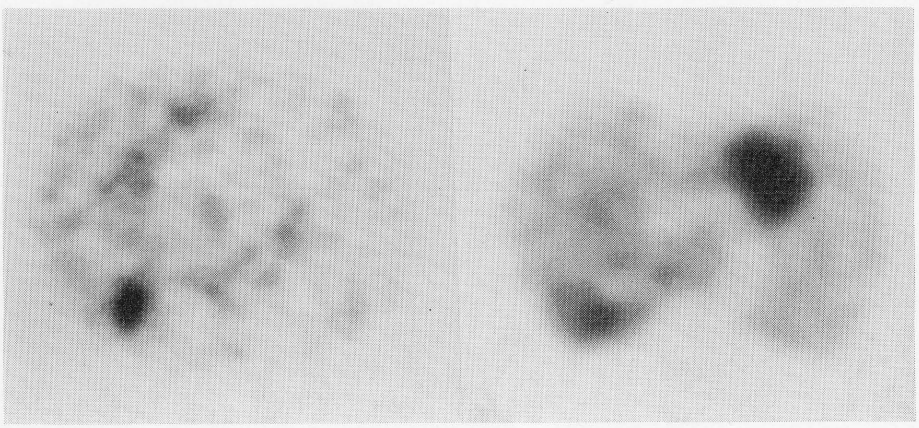

D E

Fig. 1 Images in a 80 year-old man with 4.5 cm-diameter squamous cell carcinoma of the lung (T2N0M0). A: plain chest radiograph (P-A). B: Computed tomogram. C: delayed Tl-201 SPECT. D: Ga-67 SPECT. E: delayed Tc-99m HMPAO SPECT. All SPECT images (C, D and E) shows clear demonstration of a solitary nodule in the right lower lung field, which is depicted on a chest radiograph (A) and CT scan (B).

positive rate for Ga-67 was significantly lower than that in squamous cell carcinoma and that for Tl-201 in adenocarcinoma ($p<0.05$). Tc-99m-HMPAO appeared to provide a somewhat higher positive rate of 67% in adenocarcinoma, in comparison with that of squamous cell carcinoma. Small cell carcinoma closely concentrated three different radionuclides and there was 100% sensitivity in all radionuclides. Though the results of Tl-201 SPECT confirmed a positive prediction independent of the histologic type, the positive rates in adenocarcinomas and alveolar cell carcinomas appeared to be somewhat lower than those in squamous and small cell carcinomas. Nodular size in 9 cases of Ga-67 negative adenocarcinomas ranged from 1.5 cm to 8 cm (mean: 4.0 cm) and from 2.5 cm to 7.8 cm (mean: 4.9) in 3 cases of Ga-67 positive adenocarcinomas. The low sensitivity of Ga-67 to adenocarcinoma had no relation to nodular size. Ga-67 SPECT was dominant in only one case in the visualization of multiple metastases in the ribs, whereas the primary lesion was clearly demonstrated by three radionuclide scans.

Table 3 Comparison of sensitivity of Tl-201, Ga-67 and Tc-99m-HMPAO for each histologic type

Histology	Radionuclides		
	Tl-201	Ga-67	Tc-99m-HMPAO
SCC	100% (12/12)	80% (8/10)*	50% (3/6)
Adeno	85% (11/13)**	25% (3/12)*,**	67% (4/6)
Small	100% (5/5)	100% (5/5)	100% (3/3)
Large	100% (1/1)	—	—
Alveolar	67% (2/3)	0% (0/3)	—

*,**: statistically significant ($p<0.05$)

SCC: squamous cell carcinoma, Adeno: adenocarcinoma, Small: small cell carcinoma, Large: large cell carcinoma, Alveolar: alveolar cell carcinoma

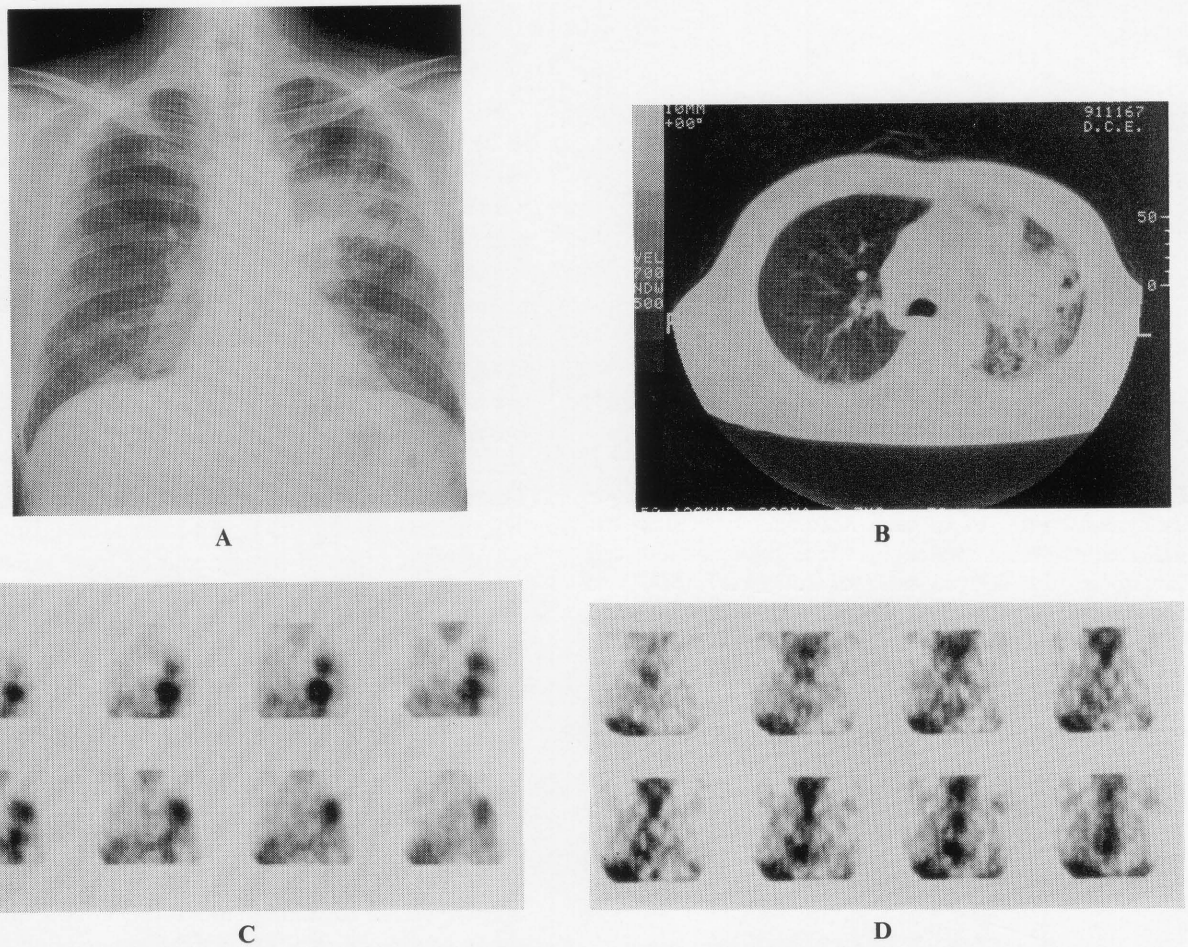

Fig. 2 Radiographic (A and B) and scintigraphic images (C and D) in a 61-year-old man with advanced adenocarcinoma of the lung (T4N3M1). A chest radiograph (A) shows a nodular shadow in the superior aspect of the left hilar region, which has infiltrative shadows into the left upper lung field. These abnormality are more obvious in a CT image (B). The coronal section image of delayed Tl-201 SPECT (C) reveals intense nodular uptake in a mass in the left upper lung field However, Ga-67 SPECT (D) does not show the abnormal uptake by the mass.

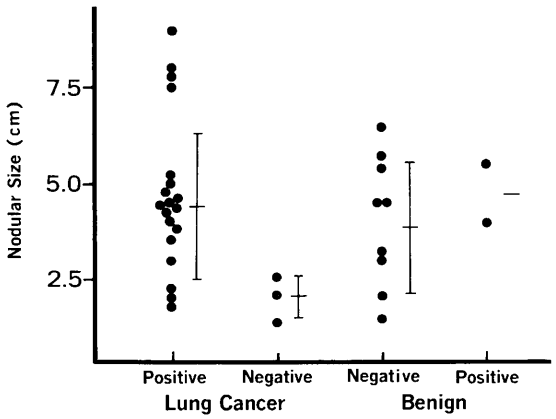

Fig. 3 Scatter plots of nodular size in positive and negative cases by Tl-201 SPECT study. The nodular size was calculated from a chest radiograph (postero-anterior projection). The bar indicates the mean±SD.

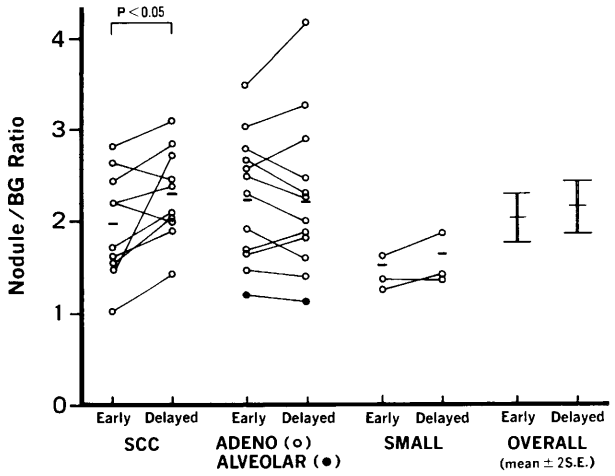

Fig. 4 Change of the early and delayed nodule-to-background ratio of in each histologic type. The bar indicates the mean value in each. In squamous cell carcinoma, the delayed ratio of 1.98±0.57 (SD) was significantly elevated than the early ratio of 2.30±0.51 ($p<0.05\%$). The early ratio is highest in adenocarcinoma.

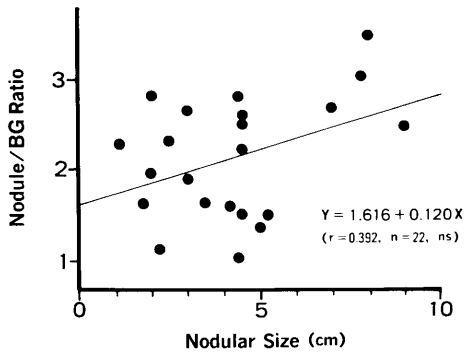

Fig. 5 Scattered diagram in function of nodular size and delayed nodule-to-background ratio in SPECT image.

Figure 3 shows the size of a nodule which was observed on CTX. The mean value for positively delineated malignant nodules was 4.44±1.99 cm (SD) in size, which was not statistically significant in comparison with the 3.83±1.74 cm of positively delineated benign nodules. Figure 4 shows the change in the Nodule/BG ratio of Tl-201 in early and delayed SPECT images. In squamous cell carcinoma, the delayed ratio was significantly increased compared to the early ratio ($p<0.05$). On the other hand, change in the uptake ratio varied in adenocarcinoma and was not significantly different in early and delayed SPECT images. The overall early ratio was 2.04±0.26 (2SE) and the delayed ratio 2.18±0.28.

The relationship between tumor size and the Nodule/BG ratio is shown in Fig. 5. The tumor uptake ratio increased as a function of size. However, no significant relationship between these two parameters was observed.

DISCUSSION

Tonami et al.[7,8] suggested that Tl-201 SPECT seems to be useful to use in differentiating malignant from benign lesions, and in the management of malignant pulmonary nodules. However, they could not compare the diagnostic values in planar and SPECT studies. In this study, Tl-201 SPECT was confirmed to improve the low sensitivity of the planar image. There are two reasons for the advantages of Tl-201 SPECT: one is the physical properties and the other the biodistribution. Tl-201 emits 69–83 keV mercury k-x-rays in 98% abundance as well as 135 keV and 167 keV gamma rays in 10% total abundance.[17] These amounts of energy are affected by tissue attenuation. When the lesion is located deep in the body, the amount of energy emitted from the uptake site is attenuated and the contrast between the target and non-target areas is impaired in the planar image. Tl-201 is primarily concentrated in the myocardium.[18] Therefore, when the lesions are located in the pericardial area and/or behind the myocardium, the uptake is also impaired in the planar image.

Experimental results have suggested that Tl-201 uptake in solid masses depends on increased vascularity, cellularity, and changes in the cell membrane.[8,19] These histopathological changes are not only specific to malignant tumors but also are observed in benign neoplasms and inflammatory lesions. Therefore, Tl-201 has been reported to be concentrated in several benign pulmonary lesions.[7,12,20] In our limited study population of benign nodules, only two cases showed false positive results. All of the negative benign lesions with Tl-201 were in a state of chronic and/or fibrotic change.

The size of a nodule did not contribute to positive delineation. Therefore, the relatively high specificity of Tl-201 might be due to the pathophysiological state of benign lesions at the time of examination. This is indicated by the fact that there are no false positive results of Ga-67 scintigraphy, because Ga-67 is known to be concentrated in active inflammatory sites.[2-4]

As an indicator for the discrimination of malignant from benign uptake, Tonami et al.[7,8] proposed the retention index (the delayed ratio minus the early ratio divided by the early ratio). When the index was high, the nodule tend to be malignant. On the other hand, in most benign nodules, early uptake was higher than delayed and the ratio of malignant to benign lesions was significantly different. Our study also showed that the relative uptake ratio in all malignant nodules tend to increase more in the delayed SPECT image than in the early image. It was also noted that differences between the early and the delayed ratios depend on the histologic type. The report by Littleton et al.[21] helps us to understand these phenomena as well as the mechanisms of Tl-201 uptake by lung cancer. He discussed the mechanism of radio-contrast enhancement in malignant and benign pulmonary lesions from the standpoint of hemodynamics in the intravascular and interstitial compartments. He suggests that a malignant tumor increases blood perfusion through the bronchial artery and decreases wash-out through the bronchial and pulmonary veins. As a result, the out-flow in an interstitial space is retarded. On the other hand, the wash-in in acute infection increases through the bronchial artery and the wash-out also increases through the veins and lymphatics. The out-flow in vascular spaces is then accelerated at the site of acute infection. It was shown by microautoradiography that injected Tl-201 is distributed in the intracellar spaces in tumor tissues.[22] If the cellular uptake of Tl-201 is related to the wash-in and the wash-out in the extracellular compartments, the intracellular retention of Tl-201 may be a function of the out-flow from the intravascular and interstitial compartments. In this context, it is understandable that delayed images may be of more use in diagnosis to discriminate acute infection from a malignant tumor.

The mechanism of Tc-99m HMPAO for tumor accumulation may have been considered to be related to the increased vascularity or blood supply.[15,16] From this point of view, Tc-99m HMPAO may be expected to be accumulated in malignant cells in the same way as Tl-201. However, Tc-99m HMPAO failed to sensitivity corresponding to Tl-201. The low sensitivity of Tc-99m HMPAO may be related to different biological properties of Tl-201: 1) Tc-99m HMPAO is distributed in the lung to a much higher degree than Tl-201. Therefore, the contrast between the nodule and the background activity is impaired. 2) The mechanism of transport of Tc-99m HMPAO through the cell membrane into the intracellular space may be only related to its lipophilicity, namely the passive diffusion. On the other hand, Tl-201 has been considered to be actively transported into viable cells by an Na^+/K^+ ATPase-exhaustive process at the cell membrane.[8,23] Differences in the transport mechanism of the two radionuclides are considered to contribute to differences in sensitivity to malignant pulmonary nodules, although the mechanism is still unclear. 3) The activity of Tc-99m HMPAO in lesions and the lung was unchanged with the function of time. In other words, no redistribution of the kind which was observed with Tl-201[24] was found at nodular sites with Tc-99m HMPAO. This evidence is not directly related to diagnostic values, but it may limit the application of Tc-99m HMPAO for the differentiation of benign from malignant lesions.

The sensitivity of Ga-67 was significantly low in adenocarcinoma. This was not expected before the study. Togawa et al.[25] found that Tl-201/Ga-67 uptake ratio (CRU) was very useful in characterizing a primary lung cancer. In his report, CRU in adenocarcinoma was higher than that in epidermoid carcinoma. These results indicate that adenocarcinoma may have low Ga-67 uptake and/or high Tl-201 uptake. The Nodule/BG ratio of Tl-201 in true positive adenocarcinoma was higher than in squamous and small cell carcinomas. The vascular beds of the extra-bronchial portion of adenocarcinoma were reported to be three times as large as those of the other types reviewed.[21] This may account for the higher Nodule/BG ratio of Tl-201 in adenocarcinoma in the early image than in squamous and small cell carcinomas. In the present study, discordant scintigraphic results for Tl-201 and Ga-67 may be helpful in characterizing a malignant nodule, particularly adenocarcinoma. Ga-67 uptake by a malignant neoplasm has been proposed to be related to transferrin receptor on the cell surface,[26,27] and may contribute to regulation of the growth of a neoplasm. The reason for the low sensitivity of Ga-67 to adenocarcinoma is not known.

In conclusion, a combination of SPECT study with Tl-201 appeared to be the best choice for predicting a malignant pulmonary nodule. The SPECT image makes it possible to overcome the physical and biological disadvantages of Tl-201 in the chest. The concentration and retention of Tl-201 in the malignant pulmonary nodule are presumed to be related to the pathophysiological characteristics of hemodynamics in malignant and benign lesions. In this context, Tl-201 SPECT may be a complementary

method to use in differentiating malignant from benign nodules which are depicted by CTX and CT.

REFERENCES

1. Wagner HN, Conti PS: Advances in medical imaging for cancer diagnosis and treatment. *Cancer* 67 (suppl. 15): 1121–1128, 1991
2. Bekerman C, Hoffer PB, Bitran JD: The role of gallium-67 in the clinical evaluation of cancer. *Semin Nucl Med* 14: 296–323, 1984
3. Bekerman C, Caride VJ, Hoffer PG, et al: Non-invasive staging of lung cancer. Indications and limitations of gallium-67 citrate imaging. *Radiol Clin North Am* 28: 497–510, 1990
4. Klech H, Kohn H, Happmann, et al: Thoracic imaging with ^{67}gallium. *Eur J Nucl Med* 13: S24–S36, 1987
5. Itoh K: Tumor scintigraphy in lung and mediastinum. In: Hisada K, Furudate M, Sasaki Y eds: *A new textbook of clinical nuclear medicine* (1st ed.). Tokyo, kanehara Shuppan, pp 241–242, 1986 (in Japanese)
6. Coleman RE: Single photon emission computed tomography and positron emission tomography in cancer imaging. *Cancer* 67 (suppl. 15): 1261–1270, 1991.
7. Tonami N, Shuke N, Yokoyama K, et al: Thallium-201 single photon emission computed tomography in the evaluation of suspected lung cancer. *J Nucl Med* 30: 997–1004, 1989
8. Tonami N, Hisada K, Watanabe Y, et al: ^{201}Tl single photon emission computed tomography in the diagnosis of lung cancer. *Rinshyo Hoshyasen* 35: 825–832, 1990 (in Japanese)
9. Sessler MJ, Geck P, Maul FD, et al: New aspects of cellular thallium uptake: Tl, Na, Cl co transport is the central mechanism of ion uptake. *Nuklearmedizin* 25: 24–27, 1986
10. Tonami N, Hisada K: Clinical experience of tumor imaging with Tl-201-chloride. *Clin Nucl Med* 2: 75–81, 1977
11. Itoh K: Study on localization of hyperfunctioning parathyroid glands by ^{201}Tl-^{99m}Tc subtraction scintigraphy. *Hokkaido Igakuzashi* 59: 701–720, 1984 (in Japanese)
12. Winzelberg GG, Hyvovitz JD: Radionuclide imaging of parathyroid tumors: historical perspectives and newer techniques. *Semin Nucl Med* 15: 161–169 1985
13. Kaplan WD, Takvorian T, Morris JH, et al: Thallium-201 brain imaging: a comparative study with pathologic correlation. *J Nucl Med* 28: 47–52, 1987
14. Neirinckx RD, Canning LR, Piper IM, et al: Technetium-99m d,l-HM-PAO: a new radiopharmaceutical for SPECT imaging of regional cerebral blood perfusion. *J Nucl Med* 28: 191–202, 1987
15. Irvine AT, Flower MA, Ott RJ, et al: An evaluation of ^{99m}Tc-HMPAO uptake in cerebral gliomas—a comparison with X-ray CT. *Eur J Nucl Med* 16: 293–298, 1990
16. Oshima M, Itoh K, Okae S, et al: Evaluation of primary lung carcinoma using technetium 99m-hexamethylpropylene amine oxime: preliminary clinical experience. *Eur J Nucl Med* 16: 859–864, 1990
17. Lebowitz E, Greene MW, Fairchild R, et al: Thallium-201 for medical use. I. *J Nucl Med* 16: 151–155, 1975
18. Bradley-Moore PR, Lebowitz E, Greene MW, et al: Thallium-201 for medical use. II: biologic behavior. *J Nucl Med* 16: 156–160, 1975
19. Ando A, Ando I, Katayama M, et al: Biodistributions of Tl-201 in tumor bearing animals and inflammatory lesions induced in animals. *Eur J Nucl Med* 12: 567–572, 1987
20. Shin W-J, Magoun S, Stopp V, et al: Thallium-201-chloride lung imaging for bronchogenic carcinoma. *J Nucl Med Tech* 2: 83–86, 1991
21. Littleton JT, Durizch ML, Moeller G, et al: Pulmonary masses: contrast enhancement. *Radiology* 177: 861–871, 1990
22. Mountz JM, Raymond PA, McKeever PE, et al: Specific localization of thallium in human high-grade astrocytoma by microautoradiography. *Cancer Res* 49: 4053–4056, 1989
23. Ando A, Ando I, Katayama M, et al: Biodistribution of radioactive alkaline metals in tumor bearing animals: comparison with ^{201}Tl. *Eur J Nucl Med* 14: 352–357, 1988
24. Pohost GM, Alpert NM, Ingwall JS, et al: Thallium redistribution: mechanism and clinical utility. *Semin Nucl Med* 10: 70–93, 1980
25. Togawa T, Suzuki A, Higuchi Y, et al: ^{201}Tl to ^{67}Ga crude uptake ratio in primary lung cancer with reference to histological type. *Haigan* 25: 187–194, 1985 (in Japanese)
26. Larson SM, Rasey JS, Allen DR, et al: Common pathway for tumor cell uptake of gallium-67 and iron-59 via a transferrin receptor. *J Natl Cancer Inst* 64: 41–53, 1980
27. Chitambar CR, Zivkovic-Gilgenbach Z: Role of acidic receptosome in the uptake and retention of ^{67}Ga by human leukemic HL60 cells. *Cancer Res* 50: 1484–1487, 1990